JOURNAL OF GEOPHYSICAL RESEARCH, VOL. 102, NO. A4, PAGES 7115–7125, APRIL 1, 1997

On estimating the amplitude of Jovian whistlers observed by Voyager 1 and implications concerning lightning

Y. Hobara, S. Kanemaru, and M. Hayakawa

Department of Electronic Engineering, The University of Electro-Communications, Tokyo, Japan

D. A. Gurnett

Department of Physics and Astronomy, University of Iowa, Iowa City

Abstract. In this paper we extensively reexamine the amplitude of many whistlers detected by the Voyager 1 and try to deduce information about the causative lightning discharges with the use of our ray-tracing computations taking into account the amplitude. As a result, we have derived the frequency spectra and mean radiation power of the causative lightning discharges and have also applied statistical method to the analysis. We can summarize our findings in the following. The average power flux spectral density of the whistlers falls in a range from $10^{-12.7}V^2m^{-2}Hz^{-1}$ to $10^{-11.0}V^2m^{-2}Hz^{-1}$. We calculated the total decrease of the whistler amplitude from the bottom of the ionosphere toward the spacecraft, as a range from about 30 to 40 dB. One of the strongest estimated lightning events exhibits a frequency dependence comparable to the terrestrial one, but its peak frequency seems to be similar to the upward current strokes on the Earth. Moreover, the rather smooth profile obtained implies a small possibility of the presence of stratified layers in the Jovian ionosphere. Other events possibly have features similar to those of the terrestrial return strokes. We calculated the mean radiation power per flash of the lightning in the Jovian atmosphere for a 1-kHz bandwidth over 60 ms, as a range from the order of 10^2 to 10^5 W. The probability distribution of the radiation power in Jupiter is found to follow a lognormal distribution, just as in the terrestrial case.

Introduction

Lightning is one of the most important electrical processes in the atmosphere of other planets such as Jupiter. Its fundamental characteristics (i.e., discharge intensity, occurrence frequency, source frequency spectra, etc.) should be investigated for the general understanding of lightning discharges and also of the atmosphere [*Scarf et al.,* 1981]. Characteristics of lightning on other planets could then be compared with those of terrestrial lightning, which has been extensively investigated [e.g., *Uman,* 1987]. Also, this kind of lightning study would be important because lightning is known to contribute to the generation of other VLF/ELF emissions as their embryonic source (see the recent review by *Hayakawa and Sazhin* [1992] for the terrestrial magnetosphere and *Wang et al.* [1995] for the Jovian magnetosphere). However, it seems that the characteristics of Jovian lightning are poorly understood; to date, because only the optical data have been utilized in deducing these characteristics [e.g., *Borucki et al.,* 1982; *Doyle and Borucki,* 1989; *Zarka,* 1985]. To our knowledge, no studies have been done in the radio frequency range based on the amplitude characteristics.

Strong evidence on the presence of lightning comes from the Voyager observations of whistlers [*Gurnett et al.,* 1979, *Kurth et al.,* 1985]. *Menietti and Gurnett* [1980] have deduced from the model calculations of ray paths that those whistlers must have originated from lightning discharges in the Jovian atmosphere. In those previous studies, however, emphasis was placed primarily on the observed dispersion characteristics. *Hobara et al.* [1995] recently considered the whistlers' amplitude characteristics; they estimated the totality of effects concerning whistler amplitude (polarization effect, focusing/defocusing effect, and collisionless (Landau and cyclotron) damping). The present paper is a further extension of our earlier study. We reestimate the intensity of nearly all the whistlers observed by the Voyager 1 spacecraft, and we try to estimate the characteristics of lightning in the Jovian atmosphere by making full use of ray-tracing, taking into account the amplitude

Paper number 96JA03996.
0148-0227/97/96JA-03996$09.00

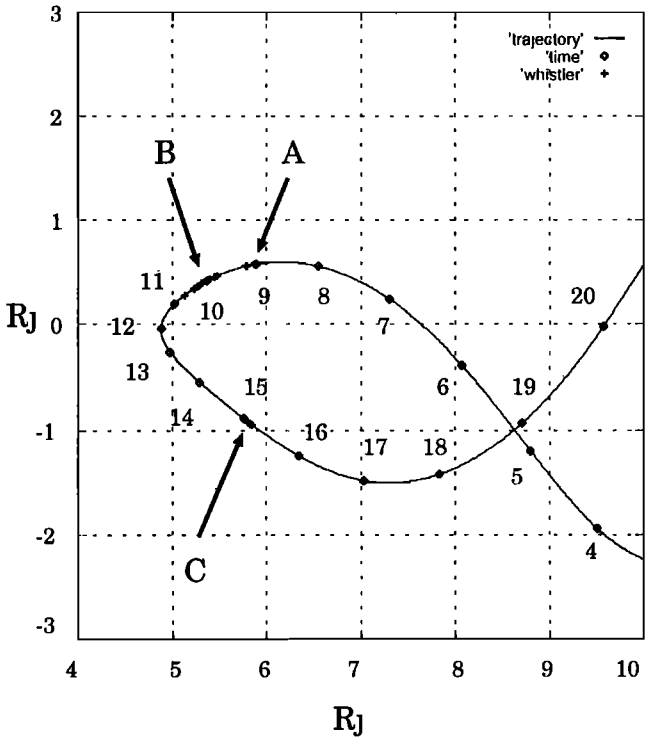

Figure 1. Trajectory of the closest approach of Voyager 1 to Jupiter. Three representative regions, A, B, and C, are indicated, where whistlers were detected. Crosses indicate the positions where the Voyager 1 PWS wideband frame (48 s) contained whistler events

information [*Hobara et al.*, 1995] together with the information obtained on whistler intensity. In this sense, the contents of this paper represent the first attempt to study the properties of lightning based on wave data obtained in the radio frequency range.

Characteristics of Lightning Whistlers in the Jovian Magnetosphere

General Properties

We have reexamined the Voyager 1 wideband waveform data with special focus on information regarding the amplitude of the lightning whistlers. About 90 whistlers were examined to determine the dispersion and upper and lower cutoff frequencies at the three different representative regions, designated A, B, and C [*Kurth et al.*, 1985]. Figure 1 shows the trajectory of Voyager 1 in the magnetic meridian plane during the closest approach on March 5, 1979. Regions A, B, and C, where the lightning-generated whistlers were detected, are also indicated in Figure 1.

Most whistlers are very weak, but 28 whistlers from the 9 wideband frames are strong enough for their power spectra to be identified as amplitude information, despite rather noisy background envelopes. As a result, the number of whistlers used in this study in the region A is 2, while there are 15 and 11 events, respectively, for B and C.

Figures 2a-2c represent examples of the dynamic spectra depicted from each region A, B, and C, respectively. The local electron gyrofrequency at the observed time is around 60.8 kHz in (Figure 2a), 80.5 kHz in (Figure 2b), and 60.7 kHz in (Figure 2c). The well-known Eckersley's approximation for the dispersion of whistlers is the relationship between the travel time, $t - t_0$ (t_0 is the time of the causative sferic) and the wave frequency f as follows:

$$t - t_0 = \frac{D}{\sqrt{f}} \text{ s Hz}^{\frac{1}{2}} \quad (1)$$

where D is a constant called "dispersion". We do not know t_0 (time of the sferics), so that we took at least three points from the dynamic spectrum of the observed whistler's trace and determine the dispersion D.

The average dispersion in region B is smallest, at about 70 s $\text{Hz}^{\frac{1}{2}}$. Larger dispersion values are observed at the other two regions. Whistlers in region A have an average dispersion of about 280 s $\text{Hz}^{\frac{1}{2}}$ and region C whistlers, about 450 s $\text{Hz}^{\frac{1}{2}}$. Though we have dealt with only a fraction of the events, these results are in good agreement with previous results [*Kurth et al.*, 1985].

Both observed dispersions and high and low cutoffs have been included among the initial conditions of our two-dimensional ray-tracing computations. These will be mentioned in the next section, in regard to determining the propagation path of whistlers from the Jovian ionosphere toward the Voyager 1 spacecraft.

Amplitude Information

The frequency spectra and absolute intensity of the whistlers were obtained by the following procedure. The peak amplitude of each whistler was estimated by the fast Fourier transform (FFT) analysis of a 60-ms sweep data of the wideband waveform. However, we cannot obtain the absolute intensity of the whistler from this data alone, without any information about the automatic gain control (AGC) gain of the receiver. So, we used the data from the 4-s scanning period of the 16-channel spectrum analyzer, along with the wideband waveform data, in order to deduce the absolute power spectral density. As a first step, we derived the frequency spectra practically averaged over 4 s of the wideband waveform data. (This variation is also used later to estimate the detection threshold of whistlers by using the background noise averaged over 4 s.) Then, we took the least squares fit with the aid of the calibrated spectral density from the 16-channel spectrum analyzer to get the amplitude differences between the two receivers, and estimated the absolute value of the wideband waveform data. During this process we assumed the background noise not to vary significantly during the 4 s. After obtaining the absolute frequency spectra of 4-s duration, we applied the same amplitude differences to the 60-ms data and tried to trace the whistler peak over its entire frequency range.

Examples of the snapshot of power spectral density averaged over 60 ms calibrated from each region, obtained in the way described above, are shown in Figures 2d-2f. These power spectra (Figures 2d to 2f)

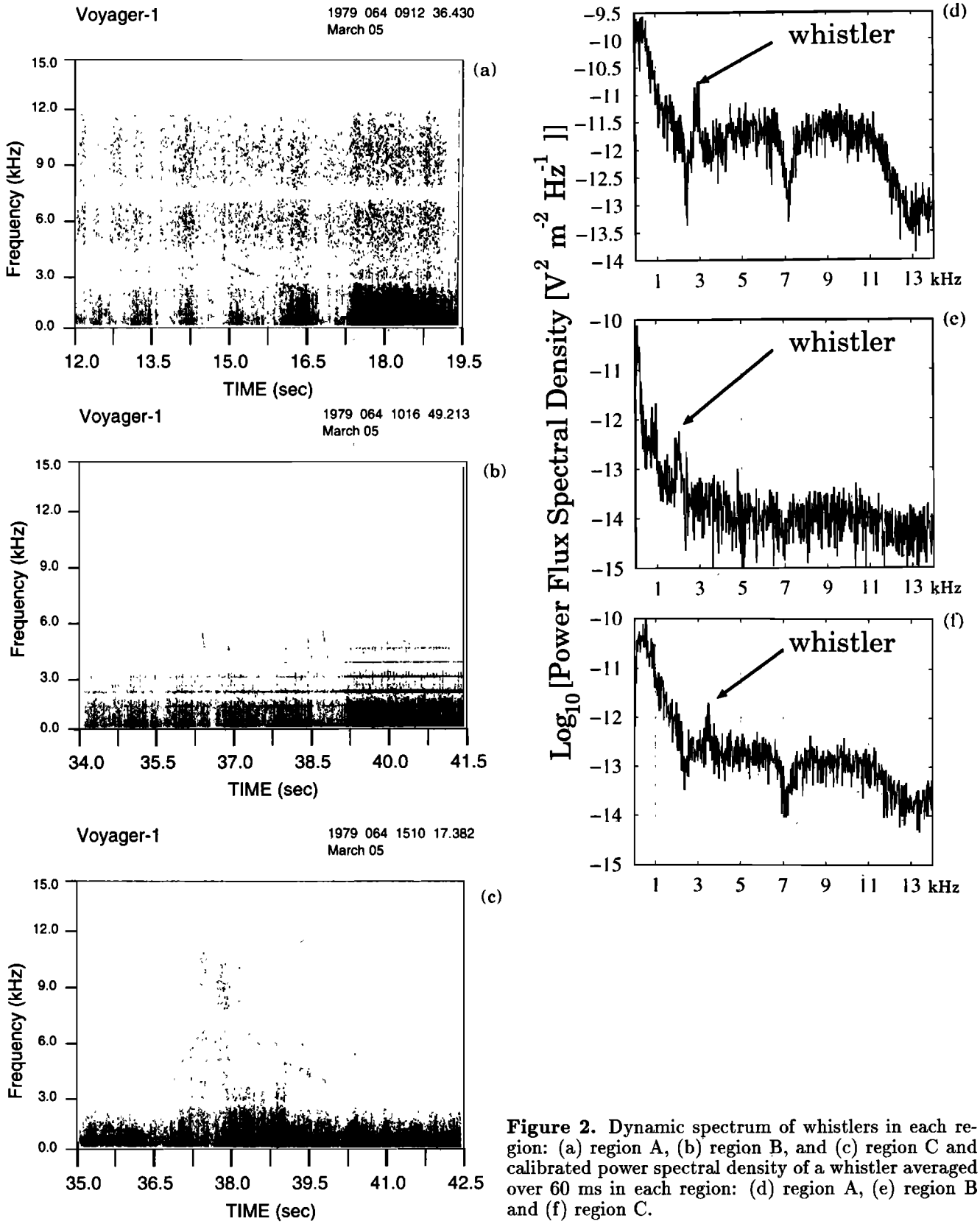

Figure 2. Dynamic spectrum of whistlers in each region: (a) region A, (b) region B, and (c) region C and calibrated power spectral density of a whistler averaged over 60 ms in each region: (d) region A, (e) region B and (f) region C.

are adopted from the events in Figures 2a to 2c respectively. Note that the time taken to produce each spectrum (60 ms) is small compared to the duration of the whole whistler and hence the lightning whistler signal in the frequency spectra appears as a very narrow band peak. The whistler signals indicated in the figures are only about 10 dB above the background noise level under the optimal conditions. Hence it seems difficult for us to trace the entire frequency range of the whistler signals, though we can detect them in the dynamic spectrum.

The detection of whistler signal is highly dependent on the variations in receiver sensitivity due to changes in the background broadband signal strength [*Kurth et al.*, 1985]. As a matter of fact, the pattern of background noise is different from one region to another. In regions A and C, the intensity of the noise during the detection of the whistler within a certain frequency range is rather high (around 10^{-12} $V^2m^{-2}Hz^{-1}$ and 10^{-13} $V^2m^{-2}Hz^{-1}$ respectively) as compared to the value in region B (about 10^{-14} $V^2m^{-2}Hz^{-1}$). The wave data show that the time variation of the difference in the background noise level between high and low rate receiver does not change significantly during detection of the whistler (maximum about 0.3 dB in A, about 1 dB in B and about 2 dB in C within a few seconds). So, the above mentioned factor does not significantly affect estimation of the whistler peak.

Another fact we must consider is the effect of a whistler-like signal on the power spectral density estimation based on FFT analysis. However, we do not have time resolution higher than 60 ms. From a practical point of view, we used the power spectral density instead of energy spectral density to estimate the mean power of the causative lightning over 60 ms in the certain frequency range, as described later, in spite of the frequency limitation. Moreover, as can be seen from their dynamic spectrum in region B, the time length (diffuseness) of a whistler is less than 50 ms in the entire frequency range and nearly the same in the other two regions. These values could be overestimated due to smoothing, and so we cannot definitely estimate how small the diffuseness of whistlers would be. However, it must be no longer than that which can be seen in the dynamic spectrum.

Now we can show the calibrated power spectral density of the whistlers, averaged over the observed frequency range for each event as a function of time (Figure 3). The error bars indicate one standard deviation from their mean value. It appears from Figure 3 that there are three clusters of events as a function of time. The group on the left side corresponds to region A, which includes two events over one wideband frame and has the largest average power flux spectral density, about $10^{-11.0}V^2m^{-2}Hz^{-1}$. Region B is located in the middle of the figure and contains 15 events over the four wideband frames. The averaged power spectral density in this region is the smallest, about $10^{-12.7}V^2m^{-2}Hz^{-1}$, and ranges from about 10^{-13} to $10^{-12}V^2m^{-2}Hz^{-1}$. The range of the power spectral density in C is found just

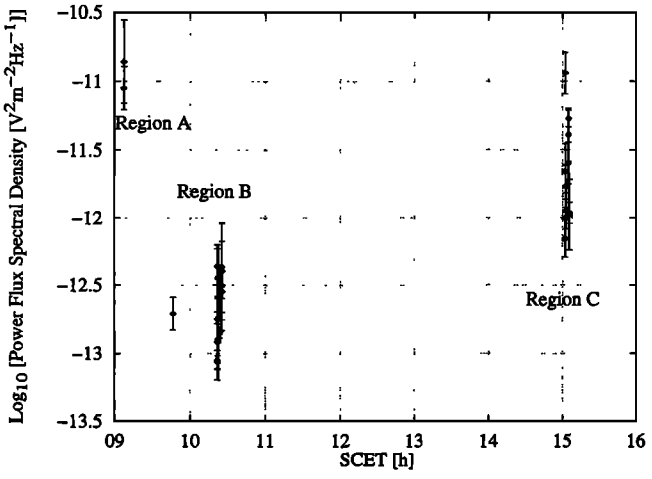

Figure 3. Temporal evolution of the whistler power spectral density averaged over the observed frequency range. SCET is spacecraft event time.

between those in the A and C and has an averaged value of $10^{-11.7}V^2m^{-2}Hz^{-1}$. There is a rather wide variation in the 11 events over the four frames. The strongest event reaches the value in A and also the smallest power spectral density is at the higher power spectral density in B. However, considering the level of the background noise as the threshold of the estimation, only the higher portion of the activities could have been detected even though the variation would expand toward the lower value.

Determination of Total Wave Amplitude Decrease of Whistlers

We used a two-dimensional ray-tracing code to estimate total attenuation through the propagation of lightning whistlers. This code takes into account the amplitude of the wave field. The essential point is to compare the variation in electric and magnetic field amplitudes caused by the changes in (1) wave polarization, (2) focusing/defocusing, and (3) kinetic collisionless damping consisting of Landau and cyclotron damping along the ray trajectory by using the continuity of Poynting flux [*Molchanov et al.*, 1995; *Hobara et al.*, 1995]. We assume the distribution function of the electrons to be isotropic Maxwellian, which means that no positive wave growth is expected. Then we estimated total wave amplitude attenuation by means of the product of these three attenuation factors.

Previous works [*Meniettı and Gurnett*, 1980; *Wang et al.*, 1995] dealt with the wave energy decrease along the wave trajectory due to Landau damping in order to analyze the propagation in the Jovian magnetosphere. From the view point of using the detected electric field strength at the Voyager spacecraft, we have to consider additional two factors (wave polarization and focusing/defocusing).

Models of the magnetic field and electron density of the Jovian magnetosphere are the same type of models as in the work of *Hobara et al.* [1995].

Ray-tracing computations were carried out with a starting altitude of 2000 km (the top of the ionosphere at night) for each 48-s PWS wideband frame data set in which the lightning whistlers were detected. The three different representative regions were identified, as mentioned earlier. To find out the paths reaching these three regions, the following procedures have been applied. First, we have assumed the reference frequency in such a way that the ray path at this frequency with the fixed initial wave normal angle (just middle between the vertical upward and the Jovian magnetic field) are computed as a function of initial Jovian magnetic latitude so as to reach the Voyager. Once the initial Jovian magnetic latitude is fixed, we compute the ray paths at different frequencies by changing their initial wave normal angles so as to reach the spacecraft. Then propagation path and the corresponding total decrease of the wave field were derived for each frame.

We will now discuss the computational results for each region, rather than for the frame. This is because the characteristics of whistlers are much more significant between the different regions as compared to the frames. In other words, they have similar properties within the same region. We obtained a rather good agreement between the two when the above condition was satisfied. This process was necessary to determine a reliable whistler propagation path. In fact, we obtained the accuracy of the estimated dispersion to the observed one about 1 percent in A and 10 percent in C averaged over each region. In the case of B, we found 30 percent accuracy averaged over the region. This discrepancy may be due mainly to the error in reading the observed frequency spectra of whistlers because of their rapid change in time and limited observed frequency range. However, the observed dispersion of the events in B which have a wider frequency range and stronger intensity is found to indicate a good agreement with that of estimated ones (accuracy within 2 percent).

Figures 4a to 4c illustrate the attenuation from three different factors (polarization, focusing/defocusing and kinetic collisionless damping) for each region A, B and C, respectively. First of all, kinetic collisionless damping consisting of Landau damping and cyclotron damping is a function of electron temperature. We vary the electron temperature ranging from T=1.0 $\times 10^5$K to T=3.0 $\times 10^5$K based on the experimental data by *Broadfoot et al.* [1979], *Scudder and Sitter* [1981], and *Divine et al.* [1983]. This is the realistic temperature range during the time where the whistlers were observed. In the case of T=1.0$\times 10^5$K, the attenuation would be negligible for all three regions, which is due mainly to a very big difference between the wave phase velocity and the net resonant electron velocity either in Landau and cyclotron damping. However, the effect for higher temperature can be noticed especially in the lower frequency in A and C. The attenuation is increased with decreasing frequency, because this would be due to the closer resonance condition for Landau damping. Nevertheless, there is no cyclotron damping in all regions and no attenuation in B for all realistic temperatures (T=1.0 to 3.0$\times 10^5$K). The difference in the attenuation from one region to another can be caused by the propagation distance between the entrance of high density torus and the spacecraft. In fact, the L value in B is smallest among the three regions, and region B is located on the edge of high density Io plasma torus. From the estimated trajectories of ray paths, we can infer that whistlers do not propagate over a large distance in the high plasma density region toward Voyager compared to other two regions (this is supported by the smallest observed dispersion).

The attenuation due to the polarization factor slightly decreases with increasing frequency (a few decibels in whole frequency considered) but is mainly constant. This tendency can be seen in all other regions. The amount of attenuation is around 10 dB in B and C, and slightly large in A (13 dB).

Finally, the contribution from the focusing/defocusing is largest among the three attenuation factors as seen from Figures 4d to 4f. The amount of attenuation is about 25 dB in A, and slightly smaller in B(22 dB), and largest in C(28 dB). The form of the variation in attenuation with frequency remains almost constant, but a small frequency variation can be seen. There is a small increase in attenuation with increasing frequency in A and a small decrease in B, while the attenuation is nearly constant up to 6 kHz and shows a sudden increase in 6.25 kHz in C. These tendencies would be brought about by the guiding effect due to the static magnetic field of Jupiter and the structure of the density profile especially in the high density Io torus.

Now, we can estimate the total attenuation by adding all three attenuation factors from the ray-tracing computations for each event (two from A, 15 and 11 events for B and C). Figures 4d to 4f represent the total decrease in electric field of the wave expected at the Voyager spacecraft. The temperature effect is significant only in the lower frequency range in A and C due to Landau damping found in Figures 4a and 4c. Except at this lower frequency, the form of the variation in attenuation with frequency remains almost constant, which is the effect of polarization and focusing/defocusing factors. However, for T=1.0$\times 10^5$K there is almost no difference in the form of the variation in attenuation with frequency among the three regions because of negligible Landau damping in all the regions. Hence, in the most frequency range all the attenuation expected at Voyager is due to the sum of polarization and focusing/defocusing factors. Amount of the attenuation is slightly different from one region to another and about 35 dB in A, 40 dB in C and 30 dB in B. As can be seen in Figures 4a to 4c, the discrepancy in the attenuation among the three regions are also due mainly to the difference in the polarization and focusing/defocusing factors.

All the ray paths treated here are of unducted propagation, and hence the observed upper frequency limit could be due to the oblique resonance in a region where f_{pe} (electron plasma frequency)$< f_{He}$ (electron gyrofrequency) and suffer from oblique resonance. In fact, the

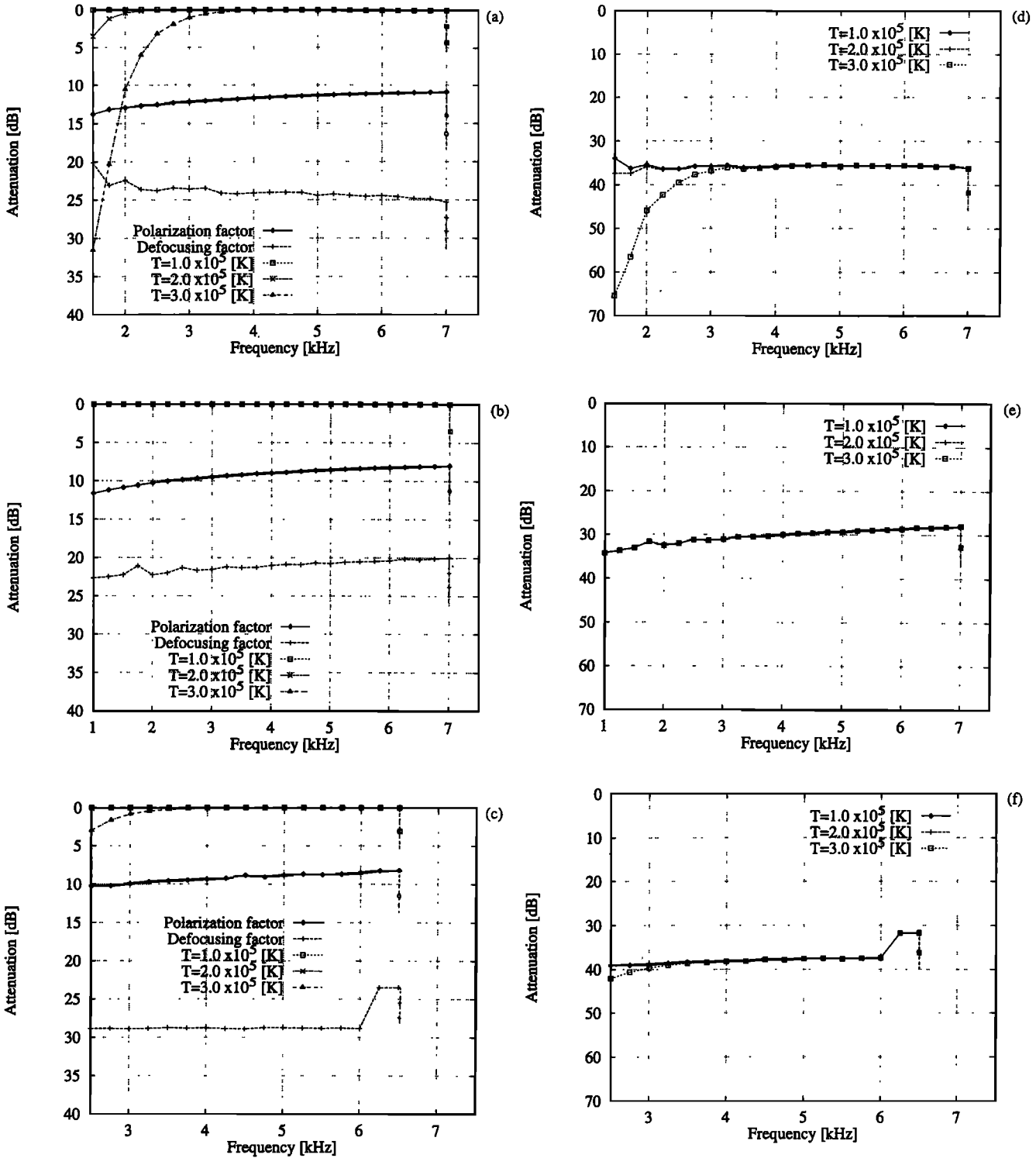

Figure 4. The attenuation from each factor in region (a) region A, (b) region B, and (c) region C. Total attenuation of the electric field of the whistler wave as a function of wave frequency for different electron temperatures (T=1.0×10^5 K to 3.0×10^5 K); (d) region A, (e) region B, and (f) region C.

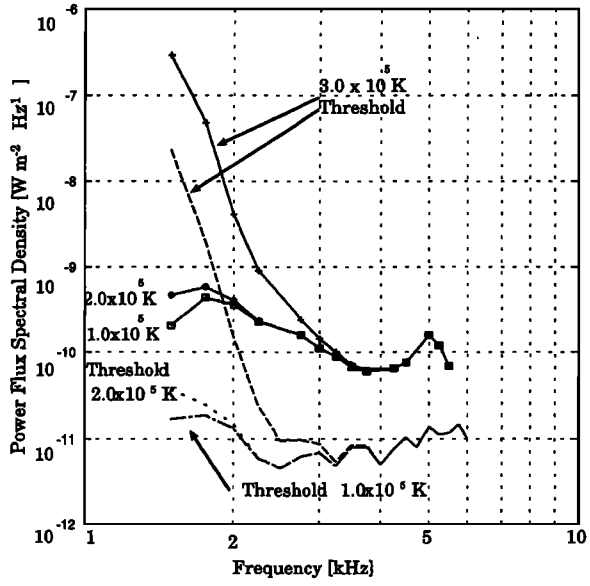

Figure 5. An example of the frequency dependence of estimated power flux spectral density (W m^{-2} Hz^{-1}) of the causative lightning (60 ms).

local f_{pe} never exceeds the corresponding f_{He} except in the high density Io torus and the ionosphere, and so the resonance causes the termination of the ray path.

Hence the upper frequency limit in Figure 4, resulting from the oblique resonance, is controlled mainly by the cold plasma density offset [see *Hobara et al.*, 1995], depending on the frame (the density offset is 1.8 cm^{-3} in A, 1.5 cm^{-3} in B and C). An alternative explanation of the observed upper frequency limit of whistlers has been proposed by *Wang et al.* [1995], who have suggested that the source location is confined to latitudes below 60° or that the power of the high-frequency whistler is below the measurable level. The difference in the explanation of the observed upper cutoff frequency is due mainly to the thermal plasma density model. The proof of the underestimation of the density in high latitudes by *Stone et al.* [1992] seems to provide a support that our model is acceptable. However, we have to state that the plasma model is still controversial because of relatively small amount of data at this region.

Among the three regions, in region C a total of 11 events were found to suffer from the strongest attenuation over the whole frequency.

Finally, we will consider the effect of the ionosphere. *Nagai et al.* [1993] have shown that an extremely large transmission loss in the Jovian ionosphere (up to 100 dB) would be expected for whistlers originating at lower latitudes for both daytime and nighttime, in contrast to a smaller transmission loss at higher latitudes (a few decibels at about 60 deg in latitude). According to our ray-tracing calculations, which assumed unducted propagation, most of the observed lightning-generated whistlers in all three regions originated from higher latitudes around 60 deg. Hence they would suffer from only a few decibels of transmission loss within the ionosphere. This means that we can ignore energy dissipation into the ionosphere.

Estimated Properties of Jovian Lightning

Now we will try to deduce the frequency spectra of causative lightning. To do this, we will add the estimated decrease in the wave amplitude during the course of propagation from the preceding ray-tracing analysis to the observed whistler frequency spectra.

Most whistlers are not sufficiently strong to yield frequency spectra in a wide frequency range. Two of the strongest event in region A, which covered a frequency range of 5 kHz can be used to examine some of the features of a causative lightning discharge. As for the other events (15 events in B and 11 events in C), their spectra were limited to a relatively narrow frequency range; also, the range of their readable frequency was different for each event. Nevertheless, we found similar characteristics within the same region. Furthermore, the notch filters in the wideband receiver are located at the frequency of 2.4 kHz and 7.2 kHz. We did not take into account the frequency spectra around these frequencies to avoid the possible underestimation of the frequency spectrum, and the estimated spectra are linearly interpolated around these frequencies.

Figure 5 illustrates the spectral density of the power flux of the causative lightning at the top of the Jovian atmosphere, from the two strongest whistlers in A. We deduced the frequency spectrum of causative lightning by adding the total attenuation (sum of three attenuation factors estimated by ray-tracing) to the corresponding frequency spectrum of the lightning whistler detected by Voyager spacecraft.

The three solid curves represent the spectrum for three different electron temperatures, T=1.0×10^5 K, T=2.0×10^5 K, and T=3.0×10^5 K. Measurement [*Broadfoot et al.*, 1979; *Scudder and Sitter*, 1981] yielded temperatures within this ranges. Also, the effective detection threshold for each temperature is shown by a dotted curve.

In Figure 5, as a general trend, the estimated power flux density increased with decreasing frequency for both the temperatures. Down to a frequency of about 3 kHz, three variations in power flux had a similar amount of $10^{-10.2}$W $m^{-2}Hz^{-1}$(60 msec average), with local peaks of $10^{-9.8}$W $m^{-2}Hz^{-1}$at about 5 kHz. But, there was a significant difference in power flux density for T=3.0×10^5 K compared to two other temperatures at frequencies lower than 3 kHz, which implies that the collisionless damping for T=3.0×10^5 K is much larger than that of T=2.0×10^5 K and T=1.0×10^5 K. Accordingly, the power flux density for T=3.0×10^5 K goes up to about $10^{-6.5}$W $m^{-2}Hz^{-1}$and $10^{-9.3}$W $m^{-2}Hz^{-1}$for T=2.0×10^5 K and $10^{-9.6}$W $m^{-2}Hz^{-1}$for T=1.0×10^5 K at 1.5 kHz.

To estimate a realistic frequency variation for causative lightning, we have to consider the effective threshold values. They are deduced from the averaged background noise during the 4 sec when a whistler is detected. For all three temperatures, the power flux density of the lightning was estimated to be around 10

dB above the threshold, at a frequency ranging from 2.5 kHz to the upper cutoff. The variation in power flux density seems to be independent of the corresponding threshold. But those two quantities of power flux density and its threshold seem to increase significantly when the frequency decreases below 2.5 kHz. The increase in threshold is due to both the increased Landau damping and the background noise level at the lower frequency. According to Figure 4a, in the cases of T=1.0×10^{5}K and T=2.0×10^{5}K, the degree of increase in Landau damping at the frequency of 4.0 kHz down to 1.5 kHz are about 0.0 dB and 3.5 dB respectively (The effect of cyclotron damping is not seen for all the frequency range we examined). In addition, frequency dependence of other two factors consisting of polarization and focusing/defocusing remain constant over this frequency range , while the increase in background noise among this frequency range is around 15 dB. Hence, the effect of Landau damping is very small in the case of T=1.0 to 2.0×10^{5}K. This fact, then, indicates that the increase in power flux density of the threshold reflects the variation in noise level. On the contrary, in the case of T=3.0×10^{5}K, the effect of Landau damping is significant and nearly 30 dB would be expected at 1.5 kHz compared to 4 kHz. In this case, Landau damping causes much larger effect toward the detection threshold than the increase in background noise in the lightning whistler's spectrum. Then the frequency dependence of the power flux is nearly identical to the frequency variation in damping. Accordingly, we took into account the signal-to-noise ratio (ratio between the background noise and the whistler signal) and the effect of whistler diffuseness in the lower-frequency range on the underestimation of power flux density. Using these, we derived the effective frequency range to characterize the frequency variation of the causative lightning discharges. Specifically, we took the frequency range of 2 to 3 kHz. We assumed the lognormal distribution represented by the relation

$$P_{\text{lightning}} \propto f^{-\alpha} \tag{2}$$

where $P_{\text{lightning}}$ is the deduced power flux spectral density of the causative lightning at the top of the Jovian atmosphere. When we take T=2.0×10^5 K, we have got "α" as 2.9, and the same value is obtained in the case of T=1.0×10^5 K, but "α =8.0" is estimated for T=3.0×10^5 K, resulting in an extremely large value of α for the frequency spectra from the lightning. *Divine et al.* [1983] indicated that the electron temperature around region A is close to T=1.0 to 2.0 ×10^5 K in the density model; and accordingly the most expectable value of coefficient a would be about 3.

The deduced frequency spectra in B are found to show a lot of fluctuations. We found the same tendency even though we averaged the spectrum over those events. Hence, we cannot detect any significant frequency dependence. As we have described for B, there is nearly a flat frequency dependence over a wide frequency range, even in the lower frequency range. So, the observed frequency spectra seem to reflect directly those of the causative lightning discharges, assuming no influence from the ionosphere (though only the strongest part of the lightning spectrum could have been detected). As the consequence of above trends, the lower cutoff frequency in B, ranging from 1.5 to 2.5 kHz implies that some of the causative lightning might have a local peak in the power spectrum at a frequency higher than the lower cutoff frequencies. In region C, both the individual event's frequency spectrum and that of the averaged one manifest the severe fluctuation feature, similar to the case of B. The situation in C is similar to that of A, which has a higher background noise and a strong estimated wave attenuation. But in contrast to region A, it does not involve an intensive event such as was observed in A. Thus, the averaged observed lower cutoff frequency is the highest among the three regions.

The existence of ledges in the ionosphere and their effects on the frequency spectrum were discussed in our previous paper [*Nagai et al.,* 1993;*Hayakawa,* 1995], which suggested an expectation of oscillating frequency dependence due to the wave interference effect of the layer. Figure 5 indicates that the frequency spectrum is rather smooth in most parts. Comparison of this figure with the corresponding frequency spectrum in *Nagai et al.* [1993] may imply that the presence of strong ledges is very unlikely in the Jovian ionosphere.

Now, we will move on to the total radiation power of Jovian lightning. The Poynting flux at the top of the Jovian atmosphere from the lightning flash $P_a(f)$ is shown as follows:

$$P_a = \int \frac{1}{T(f)^2} \frac{n_o}{Z_o} \cdot E(f)^2 \, df \tag{3}$$

where $n_0 \sim 1.0$ is the refractive index in the Jovian atmosphere, Z_o is the wave impedance of free space, and $E(f)^2$ is the spectral density of electric field strength ($V^2m^{-2}Hz^{-1}$) at the frequency f. Also, the total decrease is represented by $T(f)$. The total radiated power from the Jovian lightning flash is

$$P_{rad} = P_a 4\pi {h_i}^2 \tag{4}$$

where h_i is the height of the Jovian ionosphere taken as 150 km. We have taken the averaged radiated power for a 1-kHz bandwidth over 60 msec to compare the events, because the observed frequency range of each event is considerably different and mostly limited (up to a few kilohertz).

Figure 6 represents the mean radiated power of the Jovian lightning per flash for the bandwidth of 1 kHz, averaged over 60 ms as a function of the observation time. The error bar shows the standard deviation within the frame.

The average radiation power in region B was $10^{2.4}$ W with an accuracy of 12 percent, and in the region C, $10^{3.7}$ W with an accuracy of 15 percent. We obtained the largest value of $10^{4.8}$ W for A. Even taking into account the attenuation during the course of the propagation, there was no significant change in the relationship between the three regions as far as the power

is concerned. The estimated radiation power for each region suffered a large propagation loss of 40 dB, with a small difference (about 4 dB) between the regions, which is due mainly to the difference in the polarization and focusing/defocusing effects between the regions as can be seen in Figures 4a to 4f. as compared with the difference in the whistler power (10 to 15 dB) at the observing point. Therefore the relative importance of the estimated power between the regions is controlled mainly by the characteristics of the causative lightning discharges rather than by the propagation loss. This can be easily discerned by comparing Figure 3 with Figure 6.

In addition, the radiation power in region B is smallest, but the deviation of radiation power from the average value is not very large, nor does it extend toward a higher radiation power. Only the highest portion in B reaches the lowest part in C. This difference could be brought about by the locality of the Jovian lightning activity in the corresponding footpoint of region B. As a result, this variation may indicate the temporal or spatial locality of the lightning activity on Jupiter (especially in the longitude, because most lightning events should originate in the latitude around 60 deg). The storm in A and C could be much more active than that in B, or the altitude of the lightning discharges in B would be lower than in the other two regions by one order or so.

Finally, we tried a statistical approach to deduce the radiated power of the lightning. Figures 7a and 7b show the probability distribution of the estimated radiation power, which is the variation between the fraction of observation (percent) and the radiated power of the lightning in B and C under the electron temperature of T=3.0×10^5 K. Despite a rather small number of events, both variations seem to fit the lognormal distribution indicated by the dashed lines.

Summary and Discussion

Here we will summarize the possible characteristics of the Jovian lightning and some related inferences.

1.The average power flux spectral density of the whistlers was smallest in region B, for example, $10^{-12.7}V^2m^{-2}Hz^{-1}$ at the center frequency in the observed frequency range. The power spectral densities in regions A and C were larger, for example, $10^{-11.0}V^2m^{-2}Hz^{-1}$ and $10^{-11.7}V^2m^{-2}Hz^{-1}$, respectively. The corresponding noise level was nearly the same in most cases about 10 dB lower than the whistler signal.

2.We estimated the total decrease in amplitude of the whistlers along the propagation path by means of two-dimensional ray-tracing computations, taking into account all the amplitude factors of the wave field (focusing and defocusing, polarization, collisionless damping) for unducted propagation. The calculated total decrease of the whistler from the bottom of the ionosphere toward the spacecraft is the following: (1) region A, about 40 dB, (2) region B, about 30 dB, and (3) region C, about 35 dB. Those estimated values are principally a function of the frequency and electron temperature and we take the electron temperature for our calculation from 1.0 to 3.0×10^{5}K based on the experiment, but except at the lower-frequency range where Landau damping effect can be seen, those are almost constant.

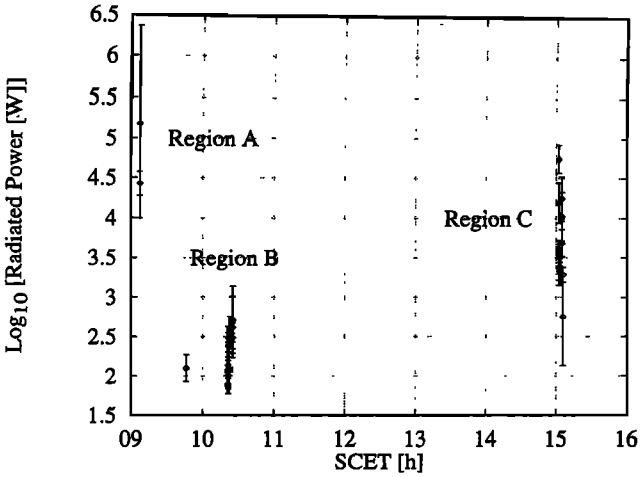

Figure 6. Estimated radiated power of the Jovian lightning as a function of time.

3.A significant difference in the frequency spectrum of the estimated lightning seems to exist between one intensive event and the weak ones. We could derive only one wideband frequency spectrum for the strongest event, which exhibits an approximate roll-off as f^{-3}. It is likely to have a peak at frequencies smaller than 1.5 kHz. Almost no frequency dependences were derived for other relatively weak events in B and C due to their highly fluctuating nature. However, the events in region B indicate that most of the local peaks occur at frequencies higher than 1.5 kHz.

4.The mean radiation power per flash of the lightning in the Jovian atmosphere for a 1 kHz bandwidth over 60 ms was calculated. It is of the order of 10^5 W in region A, 10^2 W in region B, and 10^4 W in region C. The relationships of the order of the radiation power between the three regions are based mainly on the spectral density of the whistlers, rather than on the propagation effect. In other words, this variation could be brought about by variation in the strength of the Jovian lightning activity itself. It may represent either time or space variability (especially the longitudinal variation) of the lightning activity on Jupiter.

5.The probability distribution of the radiation power in Jupiter is well described by a lognormal distribution, just as in the terrestrial case. Previous results based on optical observation of the lightning in Jupiter by *Borucki et al.* [1982] seem to support our results.

On the basis of our ray-tracing computations, we conclude that the observed events seem to originate in higher magnetic latitudes about 60 deg. Under the assumption that all the events occurring on the surface of Jupiter are taken as at a pressure of 1 bar (the same pressure as at sea level on Earth), the estimated mean

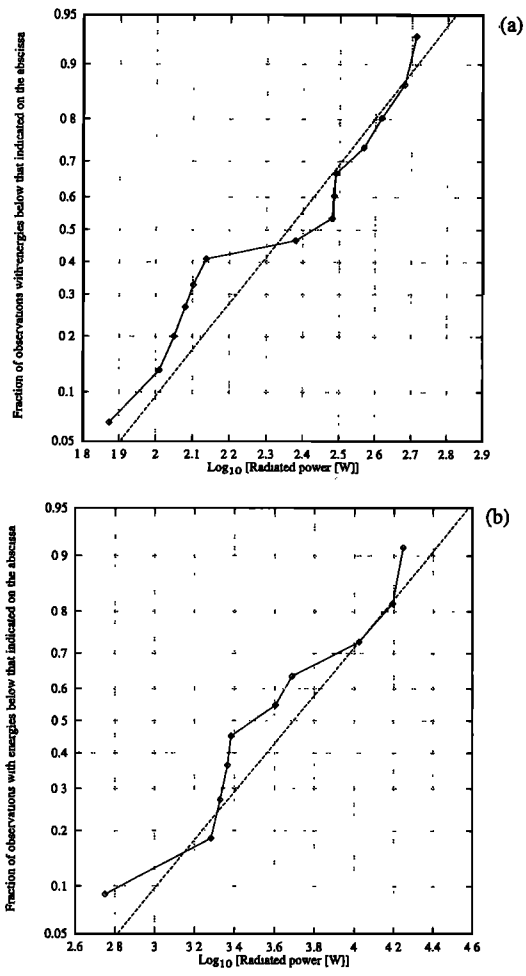

Figure 7. Cumulative fraction of radiated power of the lightning below the value shown on the abscissa; (a) region B and (b) region C.

radiated power on Jupiter (item 4) falls in a wide range from 10^2 to 10^5 W. The terrestrial lightning value of about 10^4 W for the same bandwidth, but over 200 ms [*Horner*, 1964] seems to lie within this range. A possibility is that the radiation power from the lightnings is extremely variable. Another possibility may be that even if they have nearly the same value, the location of the lightning source can differ between the regions; that is, the source location for region B might be deepest among the three regions, reflecting information about Jovian cloud structure.

On the basis of a simple comparison of the frequency spectrum of the one intensive event in A with those of many weak ones in B and C, it seems very likely that the frequency spectra of the causative lightning discharges are highly variable. We will consider about the type of lightning by examining the difference in peak frequency, which is closely related to the lightning mechanism. The typical return stroke (cloud-to-ground discharge) on Earth is known to indicate a peak frequency in the frequency spectra at about 5 kHz [*Uman*, 1987]. This characteristic does not seem to hold in the case of the one intensive event in the region A, because of its lower peak frequency. *Franz et al.* [1990] have recently demonstrated that upward current strokes have a rise time of about 10 msec and have their frequency spectrum which would have a peak at a frequency lower than 1 kHz. These features seem to fit the case of A. So, according to the frequency spectra, intensive lightning in Jupiter seems to have a similar characteristic of the upward current stroke on the Earth, even when based on the one event, while many other events in B and C (could be typical lightnings in Jupiter) are possible to have the similar feature to the terrestrial return strokes.

In addition to the radiation power in Watt (Joule per second), we are eager to estimate the total energy of each lightning flash (Joule). However, we have two serious difficulties to do this. (1) We analyzed only very narrow frequency range compared to the entire frequency range of lightning sferics, and we do not know the distribution function of the power spectral density of the causative lightning in higher frequency range. Another problem is based on their discharge process; (2)we cannot derive the exact discharge time due to the constraints of the FFT analysis even we can identify the fact that some of them must be a slow discharge process. We took each frequency spectrum averaged over 60 ms, otherwise, they became so noisy or fade. Hence here we use Watt rather than Joule to minimize an uncertainty of our estimation of the lightning property. If we could get either the ratio of total energy of the sferics to energy in the whistler frequency range in the Jovian atmosphere or entire distribution function of the power frequency spectrum of the causative lightning, and we could also get the exact discharge time, then we could have a possibility to deduce the reliable total lightning energy for sferics.

Acknowledgments. The authors are grateful to W. S. Kurth of the University of Iowa for his useful comments and suggestions and to Larry Granroth and Joe Groene for their great help in Voyager 1 PWS data analysis. We also acknowledge the Outer Planets Subnode of the Planetary Plasma Interactions of the Planetary Data System at the University of Iowa. Finally, we thank O. A. Molchanov (The University of Electro-Communications, now at University of Otago) for his useful suggestion.

The Editor thanks the referees for their assistance in evaluating this paper.

References

Borucki, W. J., A. Bar-nun, F. L. Scarf, A. F. Cook, and G. E. Hunt, Lightning activity on Jupiter, *Icarus, 52,* 492, 1982.

Broadfoot, A. L., et al., EUV observations from Voyager 1 encounter with Jupiter, *Science, 244,* 979 1979.

Divine, N., and H. B. Garrett, Charged particle distributions in Jupiter's magnetosphere, *J. Geophys. Res., 88,* 6889, 1983.

Doyle, L. R., and W. J. Borucki, Jupiter lightning locations, in *Time-Variable Phenomena in the Jovian System,* edited by M. J. S. Belton et al., p.384, NASA, Washington, D. C., 1989.

Franz, R. C., R. J. Nemzek, and J. R. Winckler, Television image of a huge cloud-to-space discharge above thunderstorm system, *Science, 249,* 48, 1990.

Gurnett, D. A., R. R. Shaw, R. R. Anderson, W. S. Kurth, and F. L. Scarf, Whistlers observed by Voyager 1: Detection of lightning on Jupiter, *Geophys. Res. Lett., 6,* 511, 1979.

Hayakawa M., Association of whistlers with lightning discharges on the Earth and on Jupiter, *J. Atmos. Terr. Phys. 57* 525, 1995.

Hayakawa M., and S. S. Sazhin, Mid-latitude and plasmaspheric hiss, A review, *Planet. Space Sci., 40,* 1325, 1992.

Hobara, Y., O. A. Molchanov, M. Hayakawa, and K. Ohta, Propagation characteristics of whistler waves in the Jovian ionosphere and magnetosphere, *J. Geophys. Res., 100,* 23523, 1995.

Horner, F., Radio noise from thunderstorms, in *Advances in Radio Research,* vol. 2, edited by J. A. Saxon, p. 121, Academic, San Diego, Calif., 1964.

Kurth, W. S., B. D. Strayer, D. A. Gurnett, and F. L. Scarf, A summary of whistlers observed by Voyager 1 at Jupiter, *Icarus, 61,* 497, 1985.

Menietti, J. D., and D. A. Gurnett, Whistler propagation in the Jovian magnetosphere, *Geophys. Res. Lett., 7,* 49, 1980.

Molchanov, O. A., O. A. Maltseva, Y. Hobara, and M. Hayakawa, A new ray tracing technique of VLF wave propagation in the Earth's magnetosphere, *Radio Sci., 30,* 1599, 1995.

Nagai, K., K. Ohta, Y. Hobara, and M. Hayakawa, Transmission characteristics of VLF/ELF radio waves through the Jovian ionosphere, *Geophys. Res. Lett., 20,* 22, 1993.

Scarf, F. L., D. A. Gurnett, W. S. Kurth, R. R. Anderson, and R. R. Shaw, An upper bound to the lightning flash rate in Jupiter's atmosphere, *Science, 213,* 684, 1981.

Scudder, J. D., and E. C. Sitter Jr., A survey of the plasma electron environment of Jupiter: A view from Voyager, *J. Geophys. Res., 86,* 8157, 1981.

Stone, R.G., et al., Ulysses radio and plasma wave observations in the Jupiter environment, *Science, 257,* 1524, 1992.

Uman, M. A., *The Lightning Discharge*, Academic, San Diego, Calif., 1987.

Wang, K., R. M. Thorne, and R. B. Horne, The propagation characteristics and Landau damping of Jovian whistlers in the Io torus, *J. Geophys. Res., 100,* 21709, 1995.

Zarka, P., On detection of radio bursts associated with Jovian and Saturnian lightning, *Astron. Astrophys., 146,* L15, 1985.

M. Hayakawa, Y. Hobara, and S. Kanemaru , Department of Electronic Engineering, The University of Electro-Communications, 1-5-1 Chofugaoka, Chofu Tokyo 182, Japan. (e-mail: yasuhide@aurora.ee.uec.ac.jp; hayakawa@whistler.ee.uec.ac.jp)

D. A. Gurnett, Department of Physics and Astronomy, University of Iowa, Iowa City, IA 52242. (e-mail: gurnett@iowave.physics.uiowa.edu)

(Received June 24, 1996; revised November 25, 1996; accepted December 11, 1996.)